World Academy of Science, Engineering and Technology
International Journal of Mechanical and Mechatronics Engineering
Vol:2, No:12, 2008

Modelling of a Direct Drive Industrial Robot

C. Pérez, O. Reinoso, N. García, J. M. Sabater, and L. Gracia

***Abstract*—** For high-speed control of robots, a good knowledge of system modelling is necessary to obtain the desired bandwidth. In this paper, we present a cartesian robot with a pan/tilt unit in end-effector (5 dof). This robot is implemented with powerful direct drive AC induction machines. The dynamic model, parameter identification and model validation of the robot are studied (including actuators). This work considers the cartesian robot coupled and non linear (contrary to normal considerations for this type of robots). The mechanical and control architecture proposed in this paper is efficient for industrial and research application in which high speed, well known model and very high accuracy are required.

***Keywords*—** Robot modelling, parameter identification and validation, AC servo-motors.

I. Introduction

FIELD oriented (or vector) control is the most popular alternating current (AC) machine control method and is widely used in high-performance industrial applications of electric drives [9][10]. In the case of an induction machine, rotor flux oriented (RFO) -see [1]- control requires an accurate value of at least some of the motor parameters in order to yield robust control [11]. The parameters which are required depends on the applied RFO control scheme.

Induction motor parameters change with temperature, frequency, and saturation [12]. The consequence of any mismatch between the parameter values used in the controller and those in the motor is that the actual rotor flux position does not coincide with the position assumed by the controller. This leads to a loss of decoupling flux and torque control. Performance of the drive therefore deteriorates from that desired. In order to avoid such a situation, it is necessary to provide the controller with accurate induction motor parameter values [1].

These AC machines are the actuators of a cartesian robot designed and manufactured for this work. This paper presents too (see section III-C) the model of a high-speed cartesian robot [3][4]. The modelling strategy take into account the robot dynamics necessary to increase the bandwidth of the servo loop, in other words, as a high speed robot we require the best possible model. We have obtained a very good model and identification of the designed robot. Obviously this paper presents a non-linear [5] and coupled model: Non-linear because discontinuous functions and inter-variable products appears in system modeling. (Equations: 14, 15, 16, 17, 20, 21, 22, 23, 26, 27, 28 and 29 are Non-Linear. Equations: 30, 31 and 32 are Quasi-Linear and finally equations: 12, 13, 18, 19, 24 and 25 are linear). Coupled because the acceleration in an axis modify the friction values in the others, so, the behavior of an axis depends of what the others are doing (This effect is modelled by equations: 14, 16, 20, 22, 26 and 28).

After modelling, robot identification is carried out and both are validated by several simulations and real experiments. Once we have the robot model, we can design a non-linear regulator to control the robot [2].

The paper is structured as follows: Section I introduces the thematic. Section II presents the Robot description; structure, characteristics, drivers and robot controller. In section III, we can find the robot modeling: sub-system equations, relationship between variables and a complete description of them. Section IV presents the parameter identification. The main contribution of this paper is the validation of this work and considerations done. In section V we present the high quality of the model and identification. Conclusions are presented in section VI and finally we can find the references.

II. Robot Description

The mechanical structure design is shown in [8] and the characteristics are: 1695 mm height, 2311 mm length and 1400 mm (see figure 1). The robot is moved by three AC servomotors (synchronous) manufactured by *SIEMENS* (1FK6 series) and with the following characteristics: for ξ and ψ axis: Torque at ω=0: 16 Nm, Nominal torque: 10.5 Nm. For ζ axe: Torque at ω=0: 11 Nm, Nominal torque: 6 Nm. *dSPACE* control card is used to implement the control algorythms (see figure 1 for mechanical and control architecture and see figures 2 and 3 for robot shape). To save data from each experiment, we have used RAM memory available in power converter transferring it to a PC via *Profibus DP*.

III. Robot Modelling

A. Model of the Induction Motor

Unfortunately, in the real world we can not find constant parameters or linear relationships. In real motors, the iron is saturated, which means that the main flux ψ_m is a function of the scalar magnetization current $i_m = |i_s + i_r|$.

Considering ψ_s and ψ_r as fluxes through the stator and the rotor windings, we can establish the relation with ψ_m, $\dot{\psi}_s$, $\dot{\psi}_r$ and motor currents as:

This work has been supported by the *Ministerio de Educación y Ciencia* of the Spanish Government through project DPI2005-08203-C02-02.

C. Pérez, O. Reinoso, N. García and J. M. Sabater are research members of the *Industrial Systems Department* of the *Miguel Hernández University*, Avda. de la Universidad S/N, 03202 Elche Spain (e-mail: carlos.perez@umh.es).

L. Gracia is research members of the *Automatic Systems Department* of the *Technical University of Valencia*, C/ Camino de Vera S/N, 46021 Valencia Spain (e-mail:luigraca@isa.upv.es).

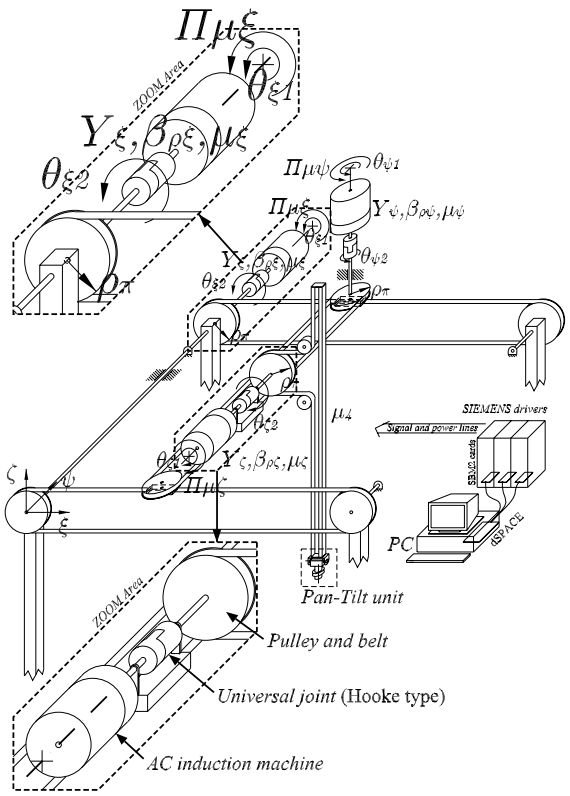

Fig. 1. Mechanical and control architecture (representation of the complete robot)

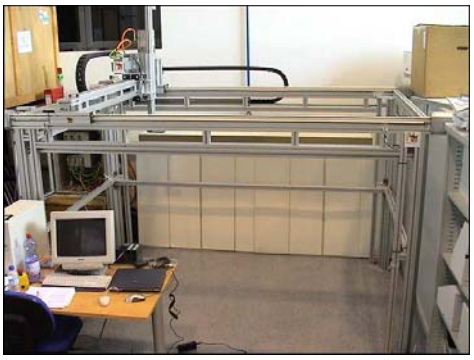

Fig. 2. Robot obtained. Photo 1. (Structure, *SIEMENS* AC induction machines and control PC with *DSPACE* card)

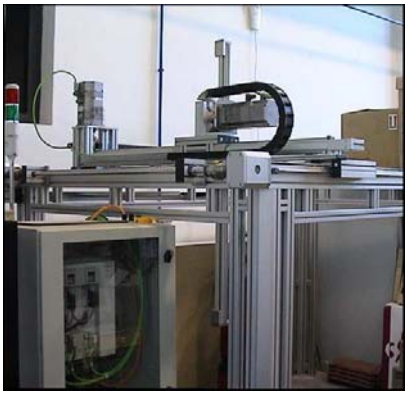

Fig. 3. Robot obtained. Photo 2. (Structure, *SIEMENS* AC induction machines and control *SIEMENS-MASTERDRIVE* drivers)

$$\psi_s = L_{sl} \cdot i_s + L_m \cdot (i_s + i_r) = L_{sl} \cdot i_s + \psi_m \quad (1)$$

$$\psi_r = L_{rl} \cdot i_r + L_m \cdot (i_s + i_r) = L_{rl} \cdot i_r + \psi_m \quad (2)$$

$$\dot{\psi}_s = -R_s \cdot i_s + u_s \quad (3)$$

$$\dot{\psi}_r - j \cdot \omega_r \cdot \psi_r = -R_s \cdot i_r \quad (4)$$

Parameter definition of the system can be found in Table I.

The currents can be calculated as a function of the stator, the rotor and the main flux.

$$i_s = \frac{1}{L_{sl}} \cdot (\psi_s - \psi_m) \quad (5)$$

$$i_r = \frac{1}{L_{rl}} \cdot (\psi_r - \psi_m) \quad (6)$$

Using equations from 1 to 6, the main flux ψ_m can be expressed by ψ_s and ψ_r:

$$\psi_s = L_{sl} \cdot i_s + L_m \cdot (i_s + i_r) \quad (7)$$

$$\psi_r = L_{rl} \cdot i_r + L_m \cdot (i_s + i_r) \quad (8)$$

Isolating ψ_m, gives the explicit expression of the main flux:

$$\psi_m = \frac{\left(\frac{1}{L_{sl}} \cdot \psi_s - \frac{1}{L_{rl}} \cdot \psi_r\right)}{\left(\frac{1}{L_m(i_m)} + \frac{1}{L_{sl}} + \frac{1}{L_{rl}}\right)} \quad (9)$$

In expression 9, the inductance L_m is a function of the magnetization current i_m, which can be calculated from the actual motor currents.

$$i_m = \sqrt{(i_{sd} + i_{rd})^2 + (i_{sq} + i_{rq})^2} \quad (10)$$

The varying inductance is determined by the magnetization current according to equation 11, which has shown to be a good approximation in practice. L_{mo} is the inductance when the iron in the motor is not saturated and i_{mo} is the current at which saturation begins. Finally, α is a factor giving the decaying curve shape of L_m at high currents.

$$L_m = \begin{cases} L_{mo} & i_m \le i_{mo} \\ \dfrac{L_{mo}}{1 + \alpha \cdot L_{mo} \cdot i_m \cdot \left(\frac{1}{i_{mo}} - \frac{1}{i_m}\right)^2} & i_m > i_{mo} \end{cases} \quad (11)$$

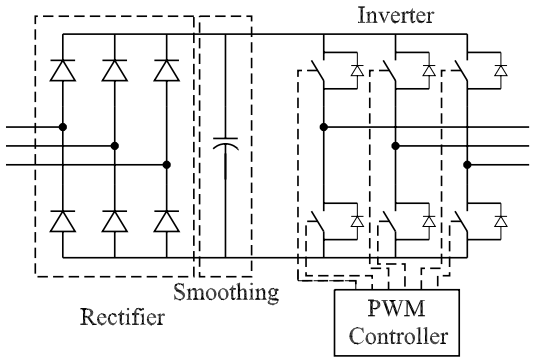

Fig. 4. Induction motor controller (rectifier, smoothing and inverter controlled by PWM. All parts are included in 1FK6 drivers)

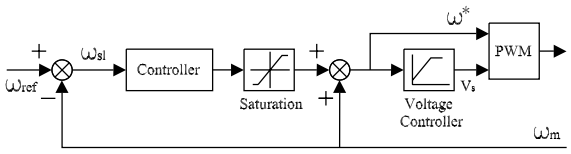

Fig. 5. Diagram of the V/Hz controller (control scheme based in steady state motor model)

The differential equation governing the dynamic behavior of the motor is given by equations 3 and 4, in which ψ_m is given in an implicit manner given by the expressions 5, 6, 9, 10 and 11. The value of ψ_m cannot be explicitly calculated for given values of ψ_s and ψ_r, but has to be approximated iteratively by a fixpoint calculation. The steps are first to assume a certain value for L_m and insert this into 9 to calculate ψ_m. Then, calculate 5 and 6 to determine i_s and i_r. Next, calculate the scalar magnetization current i_m. Finally, a new value of L_m can be calculated from the lower branch of equation 11. The exact value of ψ_m has been reached if this value is equal to the value at the beginning of the iteration cycle.
This section has been developed using the information extracted from [1] and is not our work. We have applied procedures presented in [1].

B. Converter and Controller Model

The main function of the converter is transform power supply to AC current with an specific value of frequency and voltage to be applied to the motor. Process of transformation can be divided in three steps: AC-DC conversion (rectifier), filtering (smoothing) and DC-AC conversion (inverter). We can see in figure 4 the schematic representation of induction motor controller [7].

The V/Hz control scheme is based in steady state motor model [7]. The control philosophy consists in maintaining constant the magnetic flow. We can see in figure 5 the control scheme for induction motors in our case.

C. Mechanic Model

In figure 1, a representation of the complete robot is shown. Robot modelling expressions are divided in two groups: subsystem equation and relationship between variables. These expressions represents the complete behaviour of the robot and the description of variables and constants can be found in table I (really not all variables are considered in this table, for example $\omega_{\xi 1}$ can not be found, but in equation 47, we can see the relationship with an other variable considered in the same table, Table I).

Considerations done for modelling are shown below:
- Belt transmission elasticity and shaft flexion are null;
- Inertia moments of pulleys are not considered;
- Tension of belts are not considered when no forces are applied to them.

Sub-system equations:

$$\Pi_{\mu\xi} = Y_\xi \cdot \dot{\omega}_{\xi 1} + \beta_{\rho\xi} \cdot \omega_{\xi 1} + \Pi_1 \quad (12)$$

$$\Pi_1 = \kappa_\rho \cdot (\theta_{\xi 1} - \theta_{\xi 2}) \quad (13)$$

$$R_{\rho\xi} = \kappa_{\rho 1} \cdot |\Phi_{\rho\xi 1}| + \kappa_{\rho 2} \cdot \Phi_{\rho\zeta 1} \quad (14)$$

$$\Phi_1 \cdot \rho_\Pi = aux(\Pi_1, R_{\rho\xi}, \omega_{\xi 2}) \quad (15)$$

$$R_{\lambda\xi} = \kappa_{\lambda 1} \cdot |\Phi_{\rho\psi 1}| + \kappa_{\lambda 2} \cdot |\Phi_{\rho\zeta 2} + \\ + \Phi_{\rho\zeta 3} + (\mu_{2\psi} + \mu_{2\zeta}) \cdot \gamma + \Phi_3| \quad (16)$$

$$aux(-\Phi_1, R_{\lambda\xi}, \varsigma_\xi) = (\mu_\psi + \mu_{2\psi} + \\ + \mu_\zeta + \mu_{2\zeta} + \mu_4) \cdot \dot{\varsigma}_\xi + \beta_{\lambda\xi} \cdot \varsigma_\xi \quad (17)$$

$$\Pi_{\mu\psi} = Y_\psi \cdot \dot{\omega}_{\psi 1} + \beta_{\rho\psi} \cdot \omega_{\psi 1} + \Pi_2 \quad (18)$$

$$\Pi_2 = \kappa_\rho \cdot (\theta_{\psi 1} - \theta_{\psi 2}) \quad (19)$$

$$R_{\rho\psi} = \kappa_{\rho 3} \cdot |\Phi_{\rho\psi 1}| + \kappa_{\rho 4} \cdot \Phi_{\rho\zeta 2} \quad (20)$$

$$\Phi_2 \cdot \rho_\Pi = aux(\Pi_2, R_{\rho\psi}, \omega_{\psi 2}) \quad (21)$$

$$R_{\lambda\psi} = \kappa_{\lambda 3} \cdot (\mu_\zeta + \mu_{2\zeta} + \\ + \mu_4) \cdot |\dot{\varsigma}_\xi| + \kappa_{\lambda 4} \cdot |\Phi_{\rho\zeta 3} + \mu_{2\zeta} \cdot \gamma + \Phi_3| \quad (22)$$

$$aux(\Phi_2, R_{\lambda\psi}, \varsigma_\psi) = \\ = (\mu_\zeta + \mu_{2\zeta} + \mu_4) \cdot \dot{\varsigma}_\psi + \beta_{\lambda\psi} \cdot \varsigma_\psi \quad (23)$$

$$\Pi_{\mu\zeta} = Y_\zeta \cdot \dot{\omega}_{\zeta 1} + \beta_{\rho\zeta} \cdot \omega_{\zeta 1} + \Pi_3 \quad (24)$$

$$\Pi_3 = \kappa_\rho \cdot (\theta_{\zeta 1} - \theta_{\zeta 2}) \quad (25)$$

$$R_{\rho\zeta} = \kappa_{\rho 5} \cdot |\Phi_{\rho\xi 2}| + \kappa_{\rho 6} \cdot \Phi_{\rho\zeta 3} \quad (26)$$

$$\Phi_3 \cdot \rho_\Pi = aux(\Pi_3, R_{\rho\zeta}, \omega_{\zeta 2}) \quad (27)$$

$$R_{\lambda\zeta} = \kappa_{\lambda 5} \cdot \mu_4 \cdot |\dot{\varsigma}_\xi| + \kappa_{\lambda 6} \cdot \mu_4 \cdot |\dot{\varsigma}_\psi| \quad (28)$$

$$aux\Big((\Phi_3 - \mu_4 \cdot \gamma), R_{\lambda\zeta}, \varsigma_\zeta\Big) = \\ = \mu_4 \cdot \dot{\varsigma}_\zeta + \beta_{\lambda\zeta} \cdot \varsigma_\zeta \quad (29)$$

$$\Phi_{\rho\zeta 3} = \mu_\zeta \cdot \gamma \quad (30)$$

$$\Phi_{\rho\zeta 2} = \mu_\psi \cdot \gamma \quad (31)$$

$$\Phi_{\rho\zeta 1} = \mu_\xi \cdot \gamma \quad (32)$$

In expressions (15), (16), (23), (27) and (29) the aux function is used. This function has three input variables (Π is the force or torque result, R is the dry friction and ω is the linear or angular velocity) and one output. We can find aux function definition in expression (34).

TABLE I
CONSTANT AND VARIABLE DEFINITIONS FOR SYSTEM MODELLING (MOTOR AND ROBOT)

L_{sl}, L_{rl}	stator and rotor inductance
i_s, i_r	rotor and stator currents
i_m	magnetization currents
i_{sd}, i_{rd}, i_{sq}, i_{rq}	complex currents and actual motor currents
R_s	stator resistance
u_s	applied voltage
ω_r	motor speed
$\Pi_{\mu\xi}, \Pi_{\mu\psi}, \Pi_{\mu\zeta}$	Torque generated by ξ, ψ and ζ motors respectively
$\theta_{\xi 1}, \theta_{\psi 1}, \theta_{\zeta 1}$	Angle drawee by ξ, ψ and ζ motors respectively
$\theta_{\xi 2}, \theta_{\psi 2}, \theta_{\zeta 2}$	Angle drawee by the pulley that moves each axis
Π_1, Π_2, Π_3	Torque applied to the angular springs for ξ, ψ and ζ axis
$\Phi_{\rho\xi 1}, \Phi_{\rho\psi 1}, \Phi_{\rho\zeta 4}$	Reaction forces to compensate the movement of the cart supported by the structure robot in ξ, ψ and ζ
$\Phi_{\rho\xi 2}, \Phi_{\rho\xi 3}$	Reaction horizontal forces in ζ pulleys
$\Phi_{\rho\zeta 1}, \Phi_{\rho\zeta 2}, \Phi_{\rho\zeta 3}$	Reaction vertical forces to compensate the gravity effect
$R_{\rho\xi}, R_{\rho\psi}, R_{\rho\zeta}$	Dry friction for rotation joints
$R_{\lambda\xi}, R_{\lambda\psi}, R_{\lambda\zeta}$	Dry friction for linear joints
Φ_1, Φ_2, Φ_3	Forces generated by transmission belts and pulleys for ξ, ψ and ζ axis respectively
ξ, ψ, ζ	Robot coordinate system ξ, ψ, ζ
$\mu_\xi, \mu_\psi, \mu_\zeta$	Motor mass, cart, hooke joint and pulleys for ξ, ψ and ζ
$\mu_{2\psi}, \mu_{2\zeta}$	Mass of the motor for ψ and ζ axes
μ_4	Mass of the vertical rod (ζ axis)
κ_ρ	Elastic constant of Hooke joints
$\Phi_{\rho\zeta 3}, \Phi_{\rho\zeta 4}$	Gravity effect and accelerations generated by the ζ axis
$\beta_{\rho 1}, \beta_{\rho 2}, \beta_{\rho 3}$	Rotational friction coefficients
$\beta_{\lambda 1}, \beta_{\lambda 2}, \beta_{\lambda 3}$	Translational friction coefficients
$\kappa_{\rho 1}, \ldots, \kappa_{\rho 6}$	Dry friction coefficients (rotational movements)
$\kappa_{\lambda 1}, \ldots, \kappa_{\lambda 6}$	Dry friction coefficients (lenear movements)
Φ_1, Φ_3, Φ_2	Stress forces applied to the belts
ρ_Π	Pulley radius
γ	Acceleration of gravity
Y_1, Y_2, Y_3	Inertia moment for ξ, ψ and ζ axis
Y_ξ, Y_ψ, Y_ζ	Inertia moment of ξ, ψ and ζ motors

$$\omega_{\zeta 2} = \dot{\theta}_{\zeta 2} \quad (35)$$
$$\Phi_{\rho\xi 2} = \Phi_3 \quad (36)$$
$$\Phi_{\rho\xi 3} = \Phi_3 \quad (37)$$
$$\Phi_{\rho\xi 4} = \Phi_3 \quad (38)$$
$$\omega_{\zeta 1} = \dot{\theta}_{\zeta 1} \quad (39)$$
$$\varsigma_\psi = \dot{\psi} \quad (40)$$
$$\omega_{\psi 2} = \dot{\theta}_{\psi 2} \quad (41)$$
$$\omega_{\psi 1} = \dot{\theta}_{\psi 1} \quad (42)$$
$$\varsigma_\xi = \dot{\xi} \quad (43)$$
$$\omega_{\xi 2} = \dot{\theta}_{\xi 2} \quad (44)$$
$$\Phi_{\rho\xi 1} = \Phi_1 \quad (45)$$
$$\Phi_{\rho\psi 1} = \Phi_2 \quad (46)$$
$$\omega_{\xi 1} = \dot{\theta}_{\xi 1} \quad (47)$$
$$\varsigma_\zeta = \dot{\zeta} \quad (48)$$
$$\rho_\Pi \cdot \theta_{\xi 2} = \xi \quad (49)$$
$$\rho_\Pi \cdot \theta_{\psi 2} = \psi \quad (50)$$
$$\rho_\Pi \cdot \theta_{\zeta 2} = \zeta \quad (51)$$
$$\rho_\Pi \cdot \omega_{\xi 2} = \varsigma_\xi \quad (52)$$
$$\rho_\Pi \cdot \omega_{\psi 2} = \varsigma_\psi \quad (53)$$
$$\rho_\Pi \cdot \omega_{\zeta 2} = \varsigma_\zeta \quad (54)$$
$$\rho_\Pi \cdot \dot{\omega}_{\xi 2} = \dot{\varsigma}_\xi \quad (55)$$
$$\rho_\Pi \cdot \dot{\omega}_{\psi 2} = \dot{\varsigma}_\psi \quad (56)$$
$$\rho_\Pi \cdot \dot{\omega}_{\zeta 2} = \dot{\varsigma}_\zeta \quad (57)$$

$$|\varpi| = \begin{cases} \varpi & if \quad \varpi \geq 0 \\ -\varpi & if \quad \varpi < 0 \end{cases} \quad (33)$$

$$aux(\Pi, R, \omega) = \begin{cases} \Pi - R \\ \textbf{if } (\omega > 0)\textbf{or}\big((\omega = 0) and (\Pi > R)\big) \\ \Pi + R \\ \textbf{if } (\omega < 0)\textbf{or}\big((\omega = 0) and (\Pi > -R)\big) \\ 0 \\ \textbf{if } (\omega = 0)\textbf{and}(|\Pi| < R) \end{cases} \quad (34)$$

We can find a compatible system equation in expressions from (12) to (57) with three algebraical loops and without structural singularities. We can identify expressions (14), (15), (16), (17), (20), (21), (22), (23), (26), (27), (28) and (29) as Non-Linear, expressions (30), (31) and (32) as Quasi-Linear and expressions (12), (13), (18), (19), (24) and (25) as Linear.

Non-Linear equations are introduced by *absolute value* function (see expression (33)) used to obtain the dry friction value and by aux function (see expression (34)) used to rotation and translation dynamic modelling. The problem in this case is that the *absolute value* and aux functions are discontinuous and consequently NO derivables, therefore, we can not find a linear approximation.

This system is considered coupled because the acceleration in an axis modify the friction values in the others, so, the behaviour of an axis depends on what the others are doing (This effect is modelled by expressions: (14), (16), (20), (22), (26) and (28).

For more details about modelling process, we can find in [6] an example of cartesian robot modelling.

Relationship between variables can be founded in expressions form 35 to 57.

IV. PARAMETER IDENTIFICATION

There are a lot of parameters to identify in this system. Some of them are obtained by mechanical characteristics (like masses, inertia moments), others are obtained by simply experiments (like linear frictions), manufacturer data or adjusted

TABLE II
MOTOR PARAMETER IDENTIFICATION VALUES

	ξ motor	ψ motor	ζ motor
R_s	3.181	3.02	2.76
R_r	2.55	2.61	1.66
L_{sl}	0.031	0.029	0.016
L_{rl}	0.061	0.058	0.046
L_{mo}	1.01	1.07	0.88
i_{mo}	1.11	9.66	7.33
α	0.50	0.55	0.42
J	0.019	0.018	0.012

TABLE III
ROBOT PARAMETER IDENTIFICATION VALUES

$\mu_\xi, \mu_\psi, \mu_\zeta$	=	65.32,36.15,12.75
Y_ξ, Y_ψ, Y_ζ	=	0.316,0.169,0.054
$\mu_{2\psi}, \mu_{2\zeta}, \mu_4$	=	0.324,0.152,0.846
$\kappa_\rho, \rho_\Pi, \gamma$	=	0.01224,0.225,9.8
$\beta_{\rho\xi}, \beta_{\rho\psi}, \beta_{\rho\zeta}$	=	0.323,0.398,0.190
$\beta_{1\xi}, \beta_{1\psi}, \beta_{1\zeta}$	=	0.368,0.267,0.124
$\beta_{\rho\xi}, \beta_{\rho\psi}, \beta_{\rho\zeta}$	=	0.248,0.356,0.127
$\beta_{\lambda\xi}, \beta_{\lambda\psi}, \beta_{\lambda\zeta}$	=	0.357,0.159,0.258
$\kappa_{\rho 1}, \kappa_{\rho 2}, \kappa_{\rho 3}$	=	1.172,1.146,1.938
$\kappa_{\rho 4}, \kappa_{\rho 5}, \kappa_{\rho 6}$	=	1.143,1.112,1.287
$\kappa_{\lambda 1}, \kappa_{\lambda 2}, \kappa_{\lambda 3}$	=	1.543,1.857,1.165
$\kappa_{\lambda 4}, \kappa_{\lambda 5}, \kappa_{\lambda 6}$	=	1.745,1.254,1.098

empirically, but most of them are obtained using a sequential least squares algorythm with a forgetting factor. This well known algorythm has conditioning problems when the inputs vary slowly but in our case it works properly. In [8] we can find a description of how the identification is done.
After these experiments, we obtain the values shown in tables II for the motors model and III for robot model.

V. EXPERIMENTAL RESULTS AND VALIDATION

In this section the results of several experiments are presented. One of the main parts of this work is the validation of modelling and identification process. At figures shown, we can see the high quality obtained in system modelling presented in section III, in other words, the real robot behaviour modelled in this paper is accurately modelled.

In figure 6 we can see the simulation and the real data for ξ motor torque. To obtain this figure, a step of 30 rpm input is applied (see figure 5) and the output (torque) is shown.

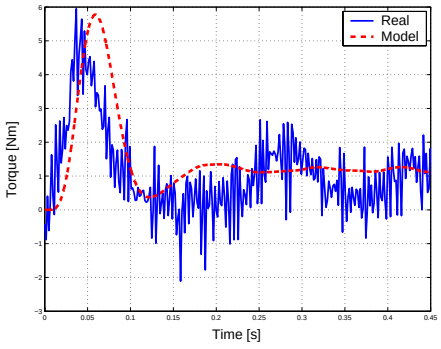

Fig. 6. Motor torque response (ξ). (RED- response of the non-linear and coupled model presented in this paper. BLUE- real response of the robot)

In figures 7, 8, 10 and 9, we can see the model and real response for several signals. For all these experiments, we plot the angular velocity of motors for a torque step input in the model described in section III-C. In all these figures we can see that the real response and the model response is quite similar.

In figure 7 we can see probably the best response obtained of all experiments done. In this figure, we can see that model (non-linear) response is exactly the same as real response. In figures like 8 and 10, we can see that model response is not exactly the same as real response every time, but in general terms is acceptable. Figures 9 and 10 show the experiments for ζ axis. We can see two experiments for this axis because they are the most complex to validate. The gravity affects the equation system shown in section III-C. Figure 9 shows the robot response for an up-moving end-effector and figure 10 shows the robot response for a down-moving. Model data of figures from 6 to 10 (simulation results) are obtained using *DYMOLA/MODELICA* but are plotted using *MATLAB*.

VI. CONCLUSION

We have presented the results and implications of our study into robot modelling, identification and model validation. In this work, we consider a complex model of the robot that allows the increase in the bandwidth of the controller. For slow or medium velocity and acceleration movements, the consideration of decoupled and linear is acceptable but for high acceleration/deceleration movements (remember that motors are 16 Nm of max torque) this type of model is needed.

One of the main differences of an industrial robot compared with lab robots is that motors are powerful, in section III-C, we present a model of the induction motors (using [1]). With this consideration, the system model is more realistic and includes the actuator allowing a very good base to obtain a control law.

So, we present a non-linear and coupled model that satisfy all specifications demanded in our case. We would like to comment on the great similarity between the model obtained in this work and real robot response.

REFERENCES

[1] R.K. Ursem, P. Vadstrup, Parameter identification of induction motors using differential evolution. *Evolutionary Computation, 2003. CEC '03.* 8-12 Dec. 2003 Volume: 2, page(s): 790- 796 Vol.2 ISBN: 0-7803-7804-0
[2] Tobias Ortmaier, Gerd Hirzinger, Cartesian control of robots with working-position dependent dynamics, *6th International IFAC Symposium on Robot Control - Syroco 2000 Sept. 21 - 23*; Vienna - Austria
[3] Sciavicco, L. And B. Siciliano, *Modeling and control of robot manipulators* (The Mc-Graw Hill Companies, 1996). ISBN: 1-85233-221-2
[4] Arthur G. Erdman, George N. Sandor, Sridhar Kota, *Mechanism Design: Analysis and Synthesis* (Prentice Hall 1996). ISBN: 0130408727
[5] Erik Wernholt, *On multivariable and nonlinear identification of industrial robots* (Linkoping Studies on Science and Technology, Thesis n. 1131).
[6] L. Gracia and C. Pérez, *Modelado de Sistemas Dinámicos. Aplicaciones* (Editorial ECU 2005). ISBN: 84-8454-422-2
[7] B.H. Rocha; M. Madrigal. Análisis del Comportamiento en Controladores de Velocidad Variable Durante Depresiones de Voltaje. *Revista IEEE América Latina. Volume:3, Issue:5, Date:Dec.2005.*
[8] C. Pérez, N. García, O. Reinoso, J. M. Azorín and R. Morales. Design, Modeling and Identification of a Cartesian Robot for Direct Visual Servoing Applications. *VIIP 2006*. Palma de Mallorca, Spain.

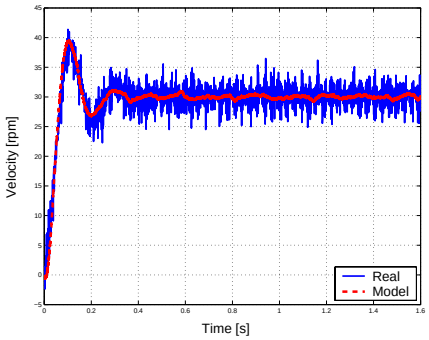

Fig. 7. Response of ξ for a step input. (RED- response of the non-linear and coupled model presented in this paper. BLUE- real response of the robot)

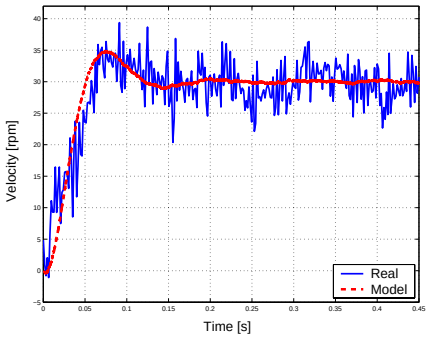

Fig. 8. Response of ψ for a step input. (RED- response of the non-linear and coupled model presented in this paper. BLUE- real response of the robot)

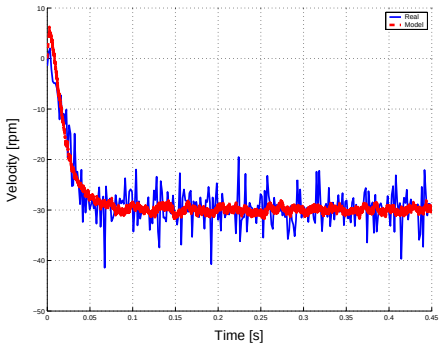

Fig. 9. Response of ζ for a step input. (RED- response of the non-linear and coupled model presented in this paper. BLUE- real response of the robot)

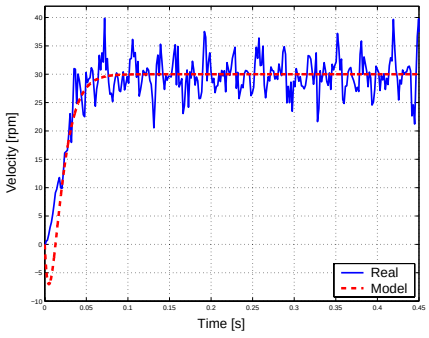

Fig. 10. Response of ζ for a step input. (RED- response of the non-linear and coupled model presented in this paper. BLUE- real response of the robot)

[9] R.D. Lorentz. Advanced Flux & Torque Control Methods for Field Oriented Induction Motor Drives. *Univ. of Wisconsin-Madison, Course Notes.*

[10] R.W. De Doncker, D.W. Novotny. The Universal Field Oriented Controller. *Conf. Rec. IEEE-IAS 88, Oct. 1988, pp. 450-456*

[11] D. Telford, M. W. Dunnigan, B. W. Williams. On-Line Identification of Induction Machine Electrical Prameters for Vector Control Loop Tuning. *IEEE Transaction on Industrial Electronics*, vol. 50, No. 2, August 2003

[12] A.B. Proca, A. Keyhani. Identification of variable frequency induction motor models from operating data. *IEEE Transactions on Energy Conversion*, vol. 17, No. 1, March 2002